Structural, electrical and optical characterization of Ti-doped ZnO films grown by atomic layer deposition

Kristin Bergum *, Per-Anders Hansen, Helmer Fjellvåg, Ola Nilsen

Centre for Materials Science and Nanotechnology (SMN), Department of Chemistry, University of Oslo, PO Box 1033, Blindern, 0315 Oslo, Norway

ABSTRACT

Thin films of Ti-doped ZnO (TZO) have been deposited using Atomic Layer Deposition (ALD) achieving highly conductive materials with resistivities down to 1.8×10^{-3} Ω cm at 1.7 cat% Ti doping, with a maximum dopant efficiency of 31%. The high conductivity and doping efficiency suggests a good distribution of dopants, otherwise a common challenge for doping by ALD. The charge mobility for Ti concentrations below 1.2 cat% was higher than for pure ZnO. The texture of the films changed from a predominantly *c*-axis to *a*-axis orientation with increasing Ti concentration, while the lattice parameters remained unaltered. The TZO films were highly transparent with an absorbance in the visible range of less than 2% for 200 nm films. The band gap increased with Ti content from 3.28 eV for pure ZnO to 3.67 eV for 5.9 cat% Ti, attributed to the Burstein Moss effect. The index of refraction varied with the Ti content showing a minimum of 1.90 for 1.7 cat% Ti.

© 2014 Elsevier B.V. All rights reserved.

1. Introduction

Transparent Conductive Oxides (TCOs) are essential components in most optoelectronic devices, and their areas of applications are ever increasing [1]. The current commercially available industrial standard ITO (Indium Tin Oxide) has excellent electronic properties ($\rho = 10^{-4}$ Ω cm), high transparencies (>90%), and a good ability for structuring [2]. However, the increasing cost and limited availability of indium is becoming a challenge in a highly competitive market. TCOs based on more abundant elements are therefore required. The current best candidate to replace ITO is doped ZnO, which has similar properties to that of ITO ($\rho = 2 \times 10^{-4}$, $T > 85\%$) [2,3]. We have chosen to use the atomic layer deposition (ALD) technique to study the deposition of doped ZnO owing to the possibilities for conformal growth on complex geometries at low deposition temperature. ALD is highly reproducible and easily scalable to an industrial process level [4].

While aluminum-doped ZnO (AZO) is by far the most investigated dopant system deposited by ALD, we have chosen titanium as a dopant due to its potential for more charges per dopant atom, and its suitable optoelectronic properties for application as an electrode, particularly in combination with H doping [2,5]. Ti-doped ZnO (TZO) has a higher work function than AZO, making it much more suitable as an anode in OLED devices than AZO and even ITO [6].

One of the challenges often encountered during aluminum doping by ALD is an uneven distribution of the dopants in the growth direction of the film [7], caused by the layer-by-layer procedure in ALD growth combined with a high aluminum growth rate. The inhomogeneous distribution may cause precipitation of dopant-rich phases even though the average composition is below the solubility limit, which is approximately 2 at% for TZO [8] and less than 3 at% for AZO [9]. This is probably one of the main reasons why AZO films produced by ALD typically has higher resistivities as compared with other deposition techniques. There have been many attempts to overcome this effect by approaches such as surface functionalization, rapid thermal annealing, under-pulsing, gas doping sequence and choice of precursor [10–14]. Studies of alternative dopants showing good optoelectronic properties, such as Ga [15], Hf [16] and Ti [17], are, however, quite limited.

The inhomogeneous dopant distribution mentioned above will be enhanced when the growth rate of the dopant oxide is fast, which is the case for the [TMA (trimethylaluminum) + H_2O] process usually used in AZO depositions. It would therefore be beneficial to choose a more slow-growing precursor combination for introduction of titanium. The process [Ti–TIP (Ti (IV) isopropoxide) + H_2O] has reported growth rates from 0.016 to 0.05 nm/cycle [18–20] at 200 °C, depending on system set-up. In our system the growth rate was measured to be 0.02 nm/cycle. This is nearly an order of magnitude less than the typical TMA growth rate of approximately 0.1 nm/cycle [21], and ought therefore to provide a better dopant distribution.

* Corresponding author.
  E-mail address: kristin.bergum@smn.uio.no (K. Bergum).

TZO has previously been reported grown by ALD by Lee et al. [17] and Ye et al. [22], using the same combination of precursors. While these studies have focused on the film properties at 50 and 100 nm thicknesses, we have focused on 200 nm thick films as the properties of the TZO films below this thickness are highly thickness-dependent. An investigation of the thickness dependent properties of TZO films deposited by the current process show that the resistivity decreases with increasing film thickness from 0.64 Ω cm for a 24 nm film and stabilize at 200 nm and above with a resistivity of 2×10^{-3} Ω cm for 3 cat% Ti. A more thorough overview of these thickness-dependent properties is under preparation. We address any discrepancies between these two studies and the current work, providing additional data for possible cross impact of the processes for deposition of ZnO and TiO$_2$. In addition, we report in depth on the evolution of crystallinity, on variations in lattice parameters and preferred orientation as well as on optical properties in the UV to IR range.

2. Experimental

Thin films of Ti-doped ZnO films were grown on single-crystalline Si (1 0 0) and soda-lime glass in a Beneq TFS-200 reactor at a deposition temperature of 200 °C. The precursors diethyl zinc (DEZ, Cambridge Chemicals, DEOX™ 99.9999%) and Ti (IV) isopropoxide (Ti–TIP, Aldrich, 97%) were delivered at 20 and 70 °C, respectively. High purity DEZ was used in order to form as pure host material as possible, while the current Ti–TIP was chosen due to its practical nature and that the majority of its impurities relates to organic fragments and chlorine, making it unlikely to affect the film properties. The oxygen reactant for both systems was deionized H$_2$O as delivered from an external container at room temperature. Titanium was introduced as dopant by altering the number of ZnO cycles between each TiO$_2$ doping layer. All films were kept as close to 200 nm as was possible. The pulse and purge times were kept constant at 0.15/0.5/0.2/0.75 s for DEZ/purge/H$_2$O/purge and 0.5/0.75/0.2/0.75 s for Ti–TIP/purge/H$_2$O/purge. The applied pulsing and purging times were verified to be well within the ALD-regime for all film depositions as no change in thickness was observed with increasing precursor pulse or purge times. The N$_2$ carrier gas (>99.999%) was supplied by a Sirocco N$_2$ generator with a combined flow rate of 550 sccm, maintaining a reactor pressure of approximately 1.3 mbar. The films have been characterized as deposited. The thickness of the films and their refractive index was determined by applying a Cauchy model to data obtained from a J.A. Woolham Alpha-SE spectroscopic ellipsometer in the interval 500–900 nm. Optical transmission and reflection spectra (200–1600 nm) were measured with a Shimatzu UV-3600 photospectrometer using an integrating sphere with compacted BaSO$_4$ powder as a reference. Both experiments were performed with an angle of 82° incident upon the film, in order to obtain the corresponding transmission and reflection data. The cation atomic composition (cat%, describes the relative molar content of the cations Ti and Zn) of the films on Si substrates were determined by X-ray fluorescence (XRF) using a Philips PW2400 XRF and analyzed by the Uniquant program. The crystal orientations, lattice parameters and crystallinity were obtained from a Bruker AXS D8 Discover powder diffractometer with a Ge(1 1 1) monochromator, providing Cu Kα_1 radiation, and detected with a LynxEye strip detector. The density was determined by means of X-ray reflectivity (XRR) data measured on a PanAlytical Empyrean diffractometer with Cu Kα_1 radiation, using a parallel beam mirror, 0.27° parallel plate collimator and a Xe proportional point detector. The electrical properties were measured using a van der Pauw Hall-type setup. The AFM images were obtained from a Park System XE-70 operated in tapping mode.

3. Results

3.1. ALD parameters

The content of Ti was controlled by varying the number of [DEZ + H$_2$O] cycles (Cy_{Zn}) before each [Ti–TIP + H$_2$O] cycle (Cy_{Ti}), changing Cy_{Zn} between 5 and 30. The resulting pulse% of Ti–TIP is described in Eq. (1).

$$\text{Pulse}\% \text{ Ti–TIP} = \frac{Cy_{Ti}}{Cy_{Ti} + Cy_{Zn}} \quad (1)$$

The evolution in average growth rate per cycle (GPC$_a$) with pulsed composition was studied over the range 0–16.7% pulsed Ti–TIP, as seen in Fig. 1. The GPC$_a$ of TZO films decreases monotonically with increasing Ti incorporation. A decrease in the average growth rate was expected as the measured GPC$_{TiO2}$ (0.02 nm/cycle)
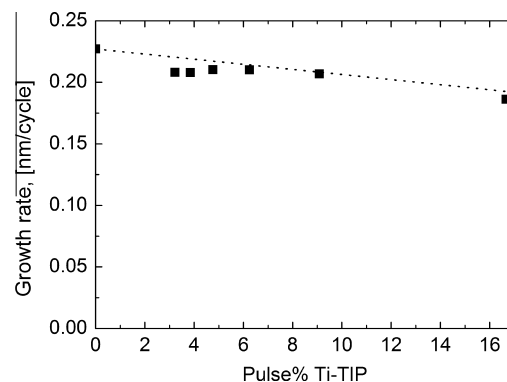

Fig. 1. Average growth rates as a function of percentage of Ti–TIP cycles. The dashed line indicates the theoretical growth rate based on the growth rates of the binary oxides.

from Ti–TIP was much less than the measured GPC$_{ZnO}$ from DEZ (0.223 nm/cycle). While the observed growth rates were slightly below the expected values, the trend is approximately as anticipated. The current observation is consistent with a slightly surface-hindered growth.

The correlation between pulsed and deposited composition is given in Fig. 2 and shows a linear relationship up to 9.1 pulse% Ti–TIP. A slight deviation is observed from the linear trend at 16.7 pulse% Ti–TIP. We observe a much higher incorporation of Ti than anticipated from the number of atoms deposited per cycle as based on the growth rates of the binary oxides and their bulk densities, shown by the dashed line in Fig. 2. The Ti concentrations vary between 0 and 5.6 cat%.

3.2. Structural characterization and morphology

The structural analyses by X-ray diffraction of the TZO films as function of Ti content can be seen in Fig. 3. All films are polycrystalline and of the hexagonal wurtzite type, and no crystalline phases of TiO$_2$ were observed. The (0 0 2) doubles in FWHM from 0.24° to 0.45° 2θ and is strongly reduced in intensity when the Ti content increases from 0 to 5.6 cat% Ti. The (1 0 0), however, decrease from 0.27° to 0.19° 2θ for 0 and 2.9 cat% Ti, respectively. At 5.9 cat%, the FWHM increase to 0.25° 2θ. This probably correlates with a change in the preferred growth direction, and thereby the shape of the crystallites. Any change in strain caused by the change in directionality might also affect the FWHM anisotropically. A more thorough comparison of (1 0 0) and (0 0 2) is seen in Fig. 4. A clear shift from a preferred orientation along the c-axis
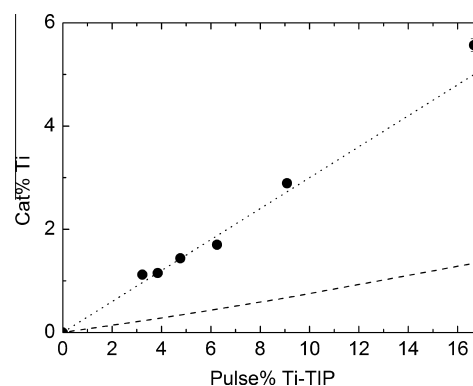

Fig. 2. Measured Ti concentration versus percentage of Ti-pulses. Dashed line indicates the theoretical concentrations based on densities and growth rates of the binary oxides; dotted line is guide to the eye.